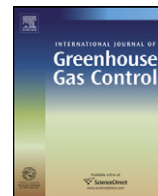Contents lists available at SciVerse ScienceDirect

International Journal of Greenhouse Gas Control

journal homepage: www.elsevier.com/locate/ijggc

Influence of the effective stress coefficient and sorption-induced strain on the evolution of coal permeability: Model development and analysis

Zhongwei Chen [a,b], Jishan Liu [a,*], Zhejun Pan [b], Luke D. Connell [b], Derek Elsworth [c]

[a] School of Mechanical and Chemical Engineering, The University of Western Australia, WA 6009, Australia
[b] CSIRO Earth Science and Resource Engineering, Private Bag 10, Clayton South, Victoria 3169, Australia
[c] Department of Energy and Mineral Engineering, Penn State University, PA 16802-5000, USA

ARTICLE INFO

ABSTRACT

A series of coal permeability experiments was conducted for coal samples infiltrated both with non-adsorbing and adsorbing gases – all under conditions of constant pressure difference between the confining stress and the pore pressure. The experimental results show that even under controlled stress conditions, coal permeability decreases with respect to pore pressure during the injection of adsorbing gases. This conclusion is apparently not congruent with our conceptual understanding: when coal samples are free to swell/shrink then no effect of swelling/shrinkage strain should be apparent on the permeability under controlled stress conditions. In this study, we developed a phenomenological permeability model to explain this enigmatic behavior of coal permeability evolution under the influence of gas sorption by combining the effect of swelling strain with that of the mechanical effective stress. For the mechanical effective stress effect, we use the concept of natural strain to define its impact on the change in fracture aperture; for the swelling strain effect, we introduce a partition ratio to define the contribution of swelling strain to the fracture aperture reduction. The resulting coal permeability model is defined as a function of both the effective stress and the swelling strain. Compared to other commonly used models under specific boundary conditions, such as Palmer–Mansoori (P–M), Shi–Durucan (S–D) and Cui–Bustin (C–B) models, our model results match the experimental measurements quite well. We match the experimental data with the model results for the correct reason, i.e. the model conditions are consistent with the experimental conditions (both are stress-controlled), while other models only match the data for a different reason (the model condition is uniaxial strain but the experimental condition is stress-controlled). We have also implemented our permeability model into a fully coupled coal deformation and gas transport finite element model to recover the important non-linear responses due to the effective stress effects where mechanical influences are rigorously coupled with the gas transport system.

© 2012 Elsevier Ltd. All rights reserved.

1. Introduction

Coal Bed Methane (CBM) is naturally occurring methane gas (CH_4) in coal seams. Methane was long considered a major problem in underground coal mining but now CBM is recognized as a valuable resource. Australia has vast reserves of coal-bed methane (about 310–410 trillion m^3) (White et al., 2005) and has attracted billions of dollars in foreign investment to develop this resource. CBM recovery triggers a series of coal–gas interactions. For gas production, the reduction of gas pressure increases effective stress which in turn closes fracture aperture and reduces the permeability (McKee et al., 1988; Seidle and Huitt, 1995; Palmer and Mansoori, 1996). As gas pressure reduces below the desorption point, methane is released from coal matrix to the fracture network and coal matrix shrinks. As a direct consequence of this matrix shrinkage the fractures dilate and fracture permeability correspondingly increases (Harpalani and Schraufnagel, 1990). Thus a rapid initial reduction in fracture permeability (due to change in effective stress) is supplanted by a slow increase in permeability (with matrix shrinkage). Whether the ultimate, long-term, permeability is greater or less than the initial permeability depends on the net influence of these dual competing mechanisms (Shi and Durucan, 2004; Chen et al., 2008; Connell, 2009). Therefore, understanding the transient characteristics of permeability evolution in fractured coals is of fundamental importance to the CBM recovery and CO_2 storage in coal, which has dual and complementary benefits: the enhanced production of methane and concurrent long-term storage of CO_2.

A broad variety of models have evolved to represent the effects of sorption, swelling and effective stresses on the dynamic

* Corresponding author. Tel.: +61 8 6488 7205; fax: +61 8 64881024.
E-mail address: jishan@cyllene.uwa.edu.au (J. Liu).

evolution of permeability over last few decades. In the latest review (Liu et al., 2011), these models are classified into two groups: permeability models under conditions of uniaxial strain and permeability models under conditions of variable stress.

Somerton et al. (1975) investigated the permeability of fractured coal to methane and presented a correlation equation in the prediction of permeability with mean stress. Gray (1987) considered the changes in the cleat permeability as a function of the prevailing effective horizontal stresses, and firstly incorporated the influence of matrix shrinkage into a permeability model. Seidle and Huitt (1995) developed a conceptual matchstick model to explain coal permeability decrease with increasing effective stress. Other stress-based coal permeability models include Harpalani and Chen (1997), Gilman and Beckie (2000), Shi and Durucan (S–D) (2004), and Cui and Bustin (C–B) (2005). Based on cubic geometry, Robertson and Christiansen (2006) described the derivation of a new equation that can be used to model the permeability behavior of a fractured, sorptive-elastic medium, such as coal, under variable stress conditions. Ma et al. (2011) proposed a permeability model based on the volumetric balance between the bulk coal, solid grains and pores, using the constant volume theory proposed by Massarotto et al. (2009).

A number of coal permeability models were developed based on strains. McKee et al. (1988) developed a theoretical permeability model using matrix compressibility as a fundamental property, but did not include the effect of sorption-induced strain on permeability change. Sawyer et al. (1990) proposed a permeability model assuming that fracture porosity (to which permeability can be directly related) is a linear function of changes in gas pressure and concentration. Palmer and Mansoori (P–M) (1996) presented a theoretical model for calculating pore volume compressibility and permeability in coals as a function of effective stress and matrix shrinkage. The P–M model was updated in Palmer et al. (2007). Similarly, the Advanced Resources International (ARI) group developed another permeability model (Pekot and Reeves, 2002). This model does not have a geomechanics framework, but instead extracts matrix strain changes from a Langmuir curve type of strain versus reservoir pressure, which is assumed to be proportional to the gas concentration curve. Zhang et al. (2008) developed a permeability model under variable stress conditions, and was extended to CO_2–ECBM conditions by (Chen et al., 2009, 2010). Connell et al. (2010) presented two analytical permeability models for tri-axial strain and stress conditions.

Pan and Connell (2007) developed a theoretical model for sorption-induced strain and applied to single-component adsorption/strain experimental data. Clarkson (2008) expanded this theoretical model to calculate the sorption-strain component of the P–M model. Pan and Connell (2011a) developed an anisotropic swelling model based on their swelling model (Pan and Connell, 2007). The dependence of coal permeability on pore volume compressibility was also investigated (Shi and Durucan, 2010; Tonnsen and Miskimins, 2010).

As reviewed above, there are a large collection of coal permeability models from empirical ones to theoretical ones. These models normally have a set of common assumptions: (1) the overburden stress remains constant; (2) coal deforms under the uniaxial strain condition; (3) the effective stress coefficient is assumed as one; and (4) the sorption-induced strain is totally counteracted by the closure of the fracture aperture. These assumptions have limited their applicability as Liu et al. (2011) concluded that current models have so far failed to explain the results from stress-controlled shrinkage/swelling laboratory tests and have only achieved some limited success in explaining and matching in situ data. Liu et al. (2011) considered the main reason for these failures is the impact of coal matrix-fracture compartment interactions has not yet been understood well and further improvements

are necessary as demonstrated in latest studies (Connell et al., 2010; Liu and Rutqvist, 2010; Izadi et al., 2011). In this study, a coal permeability model based on coal matrix-fracture interaction was developed and then implemented into a fully coupled coal deformation and gas transport finite element model to recover the important non-linear responses due to the effective stress effects.

2. Permeability model development

Previous work of Chen et al. (2011) has reported the findings of a series of experiments conducted for coal samples infiltrated both with non-adsorbing and adsorbing gases – all under conditions of constant pressure difference between the confining stress and the pore pressure. Observations have demonstrated that even under controlled stress conditions the injection of adsorbing gases actually does reduce coal permeability. The swelling strain effect has also been separated from the effective stress effect. In this section, we combined the swelling strain effect with the mechanical effective stress effect into a phenomenological permeability model to explain the enigmatic behavior of coal permeability evolution under the influence of gas sorption.

Experimental observations have shown that swelling response to the infiltration of CO_2 exhibits two key features: (1) as CO_2 infiltrates coal fracture, coal matrix swells and permeability generally reduces if the gas pressure is not very high. This occurs regardless of the mechanical constraint applied to the cracked coal sample; (2) the permeability recovers with increasing gas pressure as effective stress effects dominate in the absence of swelling-induced closure.

We use the idealized model as illustrated in Fig. 1 to represent a single fracture within a representative elementary volume. This representation is through two steps: the effective stress is applied first in a non-adsorbing medium as shown in Fig. 1(a) and then only the pore pressure in an adsorbing medium as shown in Fig. 1(b).

2.1. Evaluation of effective stress effects

In this section, we define the behavior of coal fracture where the effective stress is applied in a non-adsorbing medium. Coals are viewed as naturally fractured reservoirs with a matrix that is often assumed to have a negligible permeability in comparison to the fracture system. These fractures in coal are known as cleats with the cleat aperture sensitive to the effective stress, and increased effective stress acting to decrease the cleat aperture and thus permeability.

A number of empirical and theoretical expressions exist in the literature for describing the observed relationship between effective stress and fracture aperture (Daley et al., 2006; Liu et al., 2009).

Liu et al. (2009) argued that porous and fractured rock (or coal) is inherently heterogeneous and includes both a solid phase and pores (or fractures). Thus, an accurate description of the deformation of the rock (or coal) is important for coupled mechanical and hydrological processes, because fluid flow occurs in pores and fractures.

To deal with this issue, it is conceptualized that the fracture system has two parts, which are subject to the same stress, but follow different varieties of Hooke's law: the hard part follows the engineering-strain based Hooke's law, and the soft part obeys the natural-strain based Hooke's law, as shown in Fig. 2. This treatment is consistent with previous studies (Mavko and Jizba, 1991; Berryman, 2006; Liu et al., 2009).

Considering a fracture to be embedded into a core sample subject to a stress, σ, Hooke's law for the hard part can be expressed as

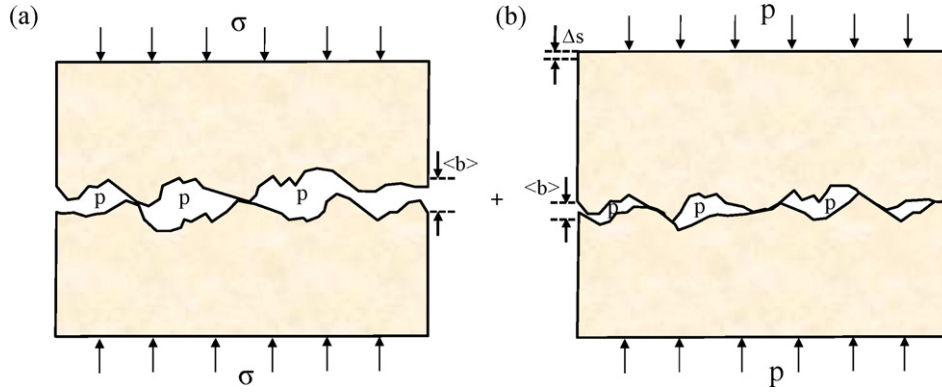$$d\sigma = K_e \cdot d\varepsilon_{b,e} \tag{1}$$

Fig. 1. Illustration of two-step loading process: (1) effective stress is applied in a non-adsorbing medium; (2) pore pressure is applied in an adsorbing medium. (a) Effective stress effects; (b) swelling strain effects. p is pore pressure, σ is overburden stress, $<b>$ is fracture aperture and Δs is sorption-induced bulk dimension change.
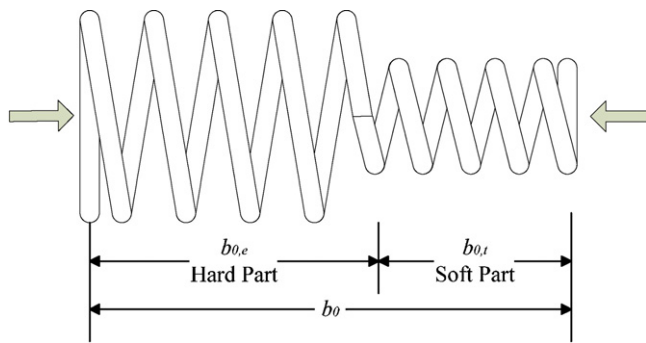

Fig. 2. Conceptualization of fracture system with the hard and soft parts. They follow engineering-strain based and natural-strain based Hooke's law, respectively. b_0 is the totally unstressed fracture aperture, $b_{0,e}$ and $b_{0,t}$ are the unstressed fracture apertures for the hard part and the soft part, respectively.

where K_e is the bulk modulus for the hard part of fracture system, and $\varepsilon_{b,e}$ is the engineering strain of fracture aperture (Jaeger et al., 2007), defined as:

$$d\varepsilon_{b,e} = -\frac{db_e}{b_{0,e}} \qquad (2)$$

where $b_{0,e}$ is the unstressed fracture aperture for the hard part. For the soft part, the following relation is used:

$$d\sigma = K_t \cdot d\varepsilon_{b,t} \qquad (3)$$

where K_t is the bulk modulus for the soft part of fracture system, and $d\varepsilon_{b,t}$ is the true or natural strain, defined as:

$$d\varepsilon_{b,t} = -\frac{db_t}{b_t} \qquad (4)$$

where b_t is the fracture aperture for soft part under the current state of stress. Subscripts e and t (for "engineering" and "true", respectively) refer to the "hard" and "soft" parts in coal fracture system.

Freed (1995) provided a historical review of the development of the concept of natural strain and argued that the natural strain should be used for accurately describing material deformation. Using the condition that $b_t = b_{0,t}$ and $b_e = b_{0,e}$ for $\sigma = 0$, the engineering strain and natural strain can be integrated into the following expressions:

$$b_e = b_{0,e}\left(1 - \frac{\Delta\sigma_e}{K_e}\right) \qquad (5)$$

$$b_t = b_{0,t}\exp\left(-\frac{\Delta\sigma_e}{K_t}\right) \qquad (6)$$

Based on the above analysis, the total fracture aperture, $<b>_{stress}$, under stressed conditions can be given as:

$$<b>_{stress} = b_e + b_t \qquad (7)$$

Combining the relation of fracture aperture change for both "hard" and "soft" parts, as shown in Eqs. (5) and (6), yields the fracture aperture change with effective stress:

$$<b>_{stress} = b_{0,e}\left(1 - \frac{\Delta\sigma_e}{K_e}\right) + b_{0,t}\exp\left(-\frac{\Delta\sigma_e}{K_t}\right) \qquad (8)$$

K_e is generally several orders larger than K_t. Therefore, the above equation can be simplified into:

$$<b>_{stress} = b_{0,e} + b_{0,t}\exp\left(-\frac{\Delta\sigma_e}{K_t}\right) \qquad (9)$$

From Fig. 2 we can see that $b_0 = b_{0,e} + b_{0,t}$, thus the following expression can be obtained.

$$<b>_{stress} = b_{0,e} + (b_0 - b_{0,e})\exp(-C_f\Delta\sigma_e) \qquad (10)$$

where C_f is coal fracture compressibility, defined as $C_f = 1/K_t$. b_0 is the initial unstressed total fracture aperture opening.

2.2. Evaluation of sorption-induced strain effects

We represent the behavior of coal permeability where fluid pressures are applied in an adsorbing medium. When the influence of swelling strain is investigated, a common way is to assume that the swelling strain is totally accommodated by the closure of fracture aperture, which could dramatically overestimate the influence of the swelling strain (Robertson, 2005; Connell et al., 2010; Liu and Rutqvist, 2010). Based on the illustration from Fig. 1, we believe that only part of total swelling strain contributes to fracture aperture change and the remaining portion of the swelling strain contributes to coal bulk deformation, and a partition factor, f, is introduced to estimate this contribution, then the fracture aperture change can be given as:

$$<b>_{swelling} = -f \times s\frac{\Delta\varepsilon_s}{3} \qquad (11)$$

where $<b>_{swelling}$ is the fracture aperture change induced by the swelling strain only, and s is the fracture spacing, f ranges from 0 to 1.0, $\Delta\varepsilon_s$ is the volumetric free swelling strain change, which can be calculated as $\varepsilon_L((p/(p+p_L)) - (p_0/(p_0+p_L)))$ with Langmuir type, as shown in Fig. 3 (Pan et al., 2011b), and $(1-f) \times s\Delta\varepsilon_s/3$ term accounts for coal bulk deformation. ε_L and p_L represent maximum volumetric swelling strain and Langmuir pressure constant, respectively.

The influence of swelling process on the internal stress distribution of coal fracture is analyzed in the following section. From
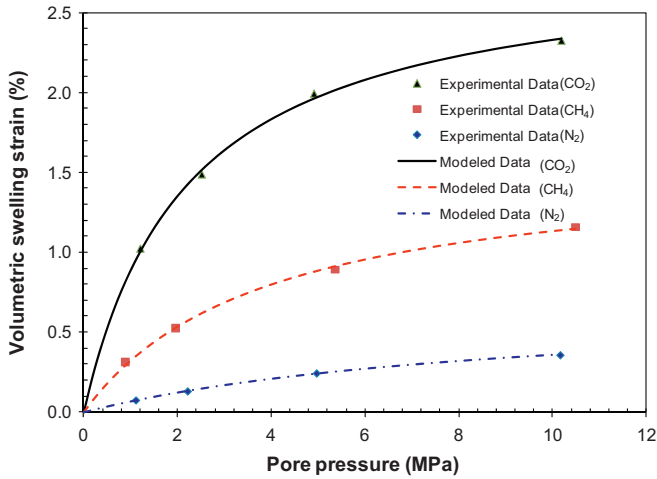
Fig. 3. Volumetric swelling strain with Langmuir type function matching: experimental data is shown with dot points, and solid line is the matching curve with Langmuir type function.

Fig. 1 we can see that after coal matrix swells, the swelling strain increases the contact area of the cleat system, and in turn closes the fracture. The cross-section of a representative element was shown in Fig. 4, where the contact area of the cleat system varies with the swelling process. Because the total stress (or confining stress) along this section is kept constant during swelling process (second stage), this internal stress along the cross section should always be balanced with surrounding boundary. Therefore, the stress balance expression is:

$$\sigma_{eb} + p \times (1 - A_b) = \sigma_{ef} + p \times (1 - A_f) \tag{12}$$

where σ_{eb} and σ_{ef} are the equivalent internal effective stress before and after swelling respectively, and A_b and A_f are the effective contact areas before and after swelling, respectively.

Because $A_b < A_f$ for the swelling case, the internal effective stress actually increases with the increase of the contact area during coal matrix swelling, as shown from Eq. (12). It was considered that the increase in effective stress is responsible for the permeability change.

2.3. Development of coal permeability model

Combining the effective stress effect (Eq. (10)) with the swelling strain effect (Eq. (11)) gives the resultant fracture aperture:

$$<b> = b_0 \left[\frac{b_{0,e}}{b_0} + \frac{(b_0 - b_{0,e})}{b_0} \exp(-C_f \Delta\sigma_e) - \frac{f}{\phi_{f0}} \times \Delta\varepsilon_s \right] \tag{13}$$

where ϕ_{f0} is the initial fracture porosity, defined as $\phi_{f0} = 3b_0/s$.

For a negligibly small residual fracture aperture ($b_{0,e} << b_0$ and $b_{0,e} \approx 0$), Eq. (13) can be simplified to:

$$<b> = b_0 \left[\exp(-C_f \Delta\sigma_e) - \frac{f}{\phi_{f0}} \times \Delta\varepsilon_s \right] \tag{14}$$

Simplifying the above equation yields:

$$<b> = b_0 [\exp(-C_f \Delta\sigma_e) - S_f \times \Delta\varepsilon_s] \tag{15}$$

where $S_f = f/\phi_{f0}$.

Based on the cubic law between aperture change and permeability (McKee et al., 1988; Seidle and Huitt, 1995), the permeability change can be expressed as:

$$\frac{k}{k_0} = \left(\frac{<b>}{b_0} \right)^3 = [\exp(-C_f \Delta\sigma_e) - S_f \times \Delta\varepsilon_s]^3 \tag{16}$$

Coal permeability model as shown in Eq. (16) can be extended to the three-dimensional case. In the analysis of coal permeability the fractured coal mass is treated as a discontinuous medium comprising both matrix and fractures (cleats). The individual matrix blocks are represented by cubes and may behave isotropically with regard to swelling/shrinkage, and mechanical deformability (Liu et al., 1999). The cleats are the three orthogonal fracture sets and may also have different apertures and mechanical properties ascribed to the different directions. Changes in coal permeability are determined by the redistribution of effective stresses or strains due to changed conditions such as gas injection. Typically, stresses and strains evolve at different rates in the different Cartesian directions, and result in anisotropic permeabilities. In simulation study, the following 3D permeability model can be implemented into numerical models:

$$\frac{k_x}{k_0} = \left(\frac{<b_x>}{b_0} \right)^3 = [\exp(-C_f \Delta\sigma_{ex}) - S_{xf} \times \Delta\varepsilon_s]^3 \tag{17a}$$

$$\frac{k_y}{k_0} = \left(\frac{<b_y>}{b_0} \right)^3 = [\exp(-C_f \Delta\sigma_{ey}) - S_{yf} \times \Delta\varepsilon_s]^3 \tag{17b}$$

$$\frac{k_z}{k_0} = \left(\frac{<b_z>}{b_0} \right)^3 = [\exp(-C_f \Delta\sigma_{ez}) - S_{zf} \times \Delta\varepsilon_s]^3 \tag{17c}$$

where b_i and σ_{ei} are the cleat opening and effective stress in i direction, respectively. $i = x, y, z$.

2.4. Physical meaning of sensitivity ratio

The initial fracture porosity, ϕ_{f0}, represents the fractured extent of the coal media, and the partition factor, f, defines the influence of both injection gas components and boundary conditions. Different gas components with different boundary conditions may have different partition magnitudes.
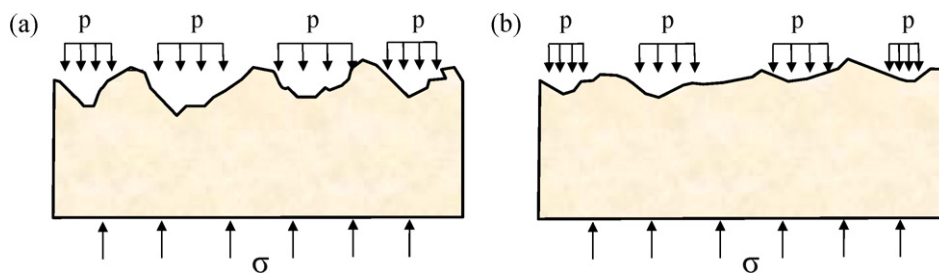

Fig. 4. Illustration of contact area change due to gas sorption: (a) pre-swelling stress state; (b) post-swelling stress state. A_b and A_f are the effective contact areas before and after swelling, respectively.

In order to explain the physical meaning of the new parameter, S_f, the fracture strain change, $\Delta\varepsilon_{bs}$, induced by coal swelling only is defined as:

$$\Delta\varepsilon_{bs} = \frac{<b>_{swelling}}{b_0} = -S_f \times \Delta\varepsilon_s \qquad (18)$$

This can be simplified into:

$$S_f = -\frac{\Delta\varepsilon_{bs}}{\Delta\varepsilon_s} = -\frac{\Delta\varepsilon_{bs}}{\varepsilon_{sf} - \varepsilon_{s0}} \qquad (19)$$

where ε_{sf} is the volumetric free swelling strain at the final stage, and ε_{s0} is the volumetric free swelling strain at the initial stage.

Therefore, S_f represents the ratio of fracture strain change to the incremental volumetric swelling strain, defined as a sensitivity ratio in this study. If the boundary conditions are the same, a larger S_f value means that cleat aperture change is more sensitive to sorption-induced strain. In our experimental tests, S_f varies from 6.82 to 54.8.

3. Permeability model evaluation

A series of gas flow-through experiments have been carried out all under constant pressure difference conditions (Chen et al., 2011), which were defined as the difference between confining stress and pore pressure. First, the effective stress coefficient is measured for the non-adsorbing gas (helium) flow-through experiments. In these experiments, the impact of gas sorption is null and any permeability alteration is considered to be due to the variation in the effective stress coefficient. Second, the change in permeability resulting from the non-adsorbing gas experiments is used to calibrate the subsequent experiments using adsorbing gases (CO_2 and CH_4) where the effect of sorption-induced strain alone, on permeability change, is obtained. The measured two sets of corrected data (core No. 01 and No. 02) and another two sets of experimental data from core Anderson 01 (Robertson and Christiansen, 2007) and core Sulcis Coal (Pini et al., 2009) were used to evaluate the newly developed permeability model in this work. Values of the volumetric swelling parameter as listed in Table 1 were taken directly from these references. These values were obtained through matching experimental data with the Langmuir curve type of strain versus pore pressure (Robertson and Christiansen, 2007).

3.1. Permeability model verification

Model results were compared with experimental data for cores No. 01 and No. 02. Effects of sorption-induced strain alone on permeability change were investigated in this comparison. In this comparison, only the sensitivity ratio, S_f, is adjustable in this match, and matching results are shown in Figs. 5 and 6.

Both data matches verify the validity of this newly developed coal permeability model. It can be seen that the sensitivity ratio, S_f, increases with the effective stress. This observation indicates that under a higher effective stress, larger fracture opening change is induced, and a small change of fracture aperture could cause a dramatic change in the $<b>_{swelling}/b_0$ ratio.

3.2. Comparison with other permeability models

In this section, experimental data from core Anderson 01 (Robertson and Christiansen, 2007) and core Sulcis Coal (Pini et al., 2009) were used to compare this developed permeability model with other widely used permeability models, including updated Palmer–Mansoori (P–M) model, Shi–Durucan (S–D) model, Cui–Bustin (C–B) model (Shi and Durucan, 2004; Cui and
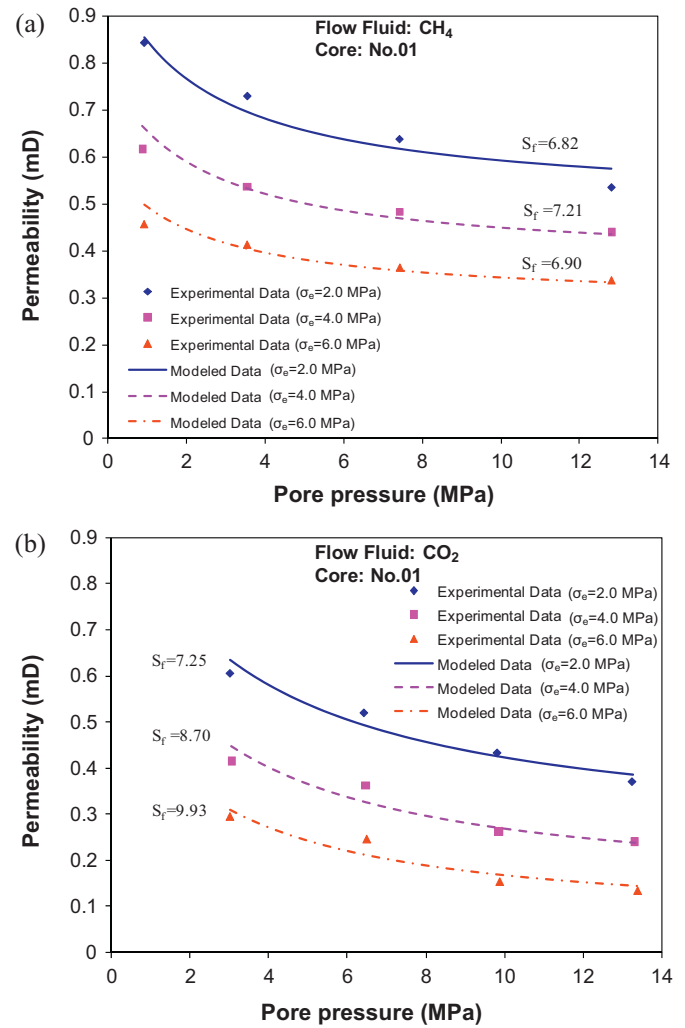
Fig. 5. Comparisons of experimental permeability with the model results for core No. 01: (a) adsorbing gas CH_4; (b) adsorbing gas CO_2.

Bustin, 2005; Palmer et al., 2007). For coal Anderson 01, experimental data for CO_2 and CH_4 were chosen. The confining pressure was 6.895 MPa (1000 psi) for all experiments, and injection pressure varied from 0.5 MPa to 5.6 MPa. For Sulcis Coal, the confining
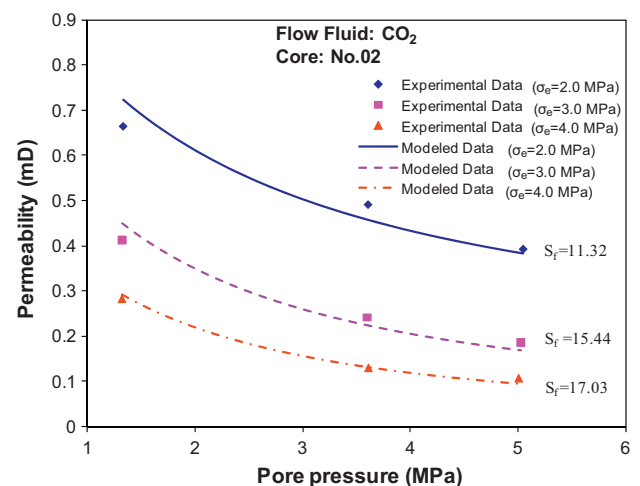
Fig. 6. Comparison of experimental permeability with the modeled results for core No. 02.

Table 1
Parameter values obtained from experimental data matching.

Parameter	Core No. 01	Core No. 02	Anderson 01	Sulcis coal
Langmuir strain constant for CO_2 (%)	0.052	0.045	0.0353	0.049
Langmuir pressure constant for CO_2 (MPa)	5.20	3.20	3.83	7.25
Langmuir strain constant for CH_4 (%)	0.030	–	0.0168	–
Langmuir pressure constant for CH_4 (MPa)	2.96	–	6.11	–

stress was 10.0 MPa and the injection pressure increased from 0.49 to 7.75 MPa. These comparisons are to benchmark the performance of our model against others.

Coal swelling parameters from laboratorial tests were used, as listed in Table 1. Because the cleat compressibility was not given in both references, both the fracture compressibility and the sensitivity ratio, S_f, were considered as the variables for our permeability model. For other permeability models, the physical properties of Young's modulus and Poisson's ratio are recovered directly from the experiments (Robertson and Christiansen, 2007; Pini et al., 2009), and fracture compressibility was considered to be variable for both S–D model and C–B model. Fracture porosity is the matching parameter for P–M model. The best matching parameters for each model are listed in Table 2, and the comparison results are shown in Figs. 7 and 8.

For the compared permeability models, as shown in Figs. 7 and 8, the total swelling strain is used to calculate permeability variation. The experimental data show that sorption-induced strain only plays a dominant role at low pressures (permeability reduction), as shown in Figs. 7 and 8, and the pore pressure induced effective stress change takes over the dominant role (permeability increase) at higher pore pressures. Therefore, these models are not capable of replicating this apparently anomalous behavior if the total swelling strain data are adopted since the uniaxial-strain assumption is used in these models while the experimental conditions are not uniaxial strain.

For our model, we considered that only part of the total swelling strain contributes to the cleat aperture change, while the remaining part contributes to coal bulk deformation. The effect of swelling strain on permeability change is evaluated by a partition factor, as defined in Eq. (11). We believe that this assumption adequately reflects the mechanism for the interaction between coal swelling strain and permeability change, and that is why this developed model is capable of replicating this behavior.

In order to better explain this model, the relationship between cleat porosity and the partition ratio of total swelling strain contributing to cleat aperture change was listed and plotted in Table 3 and Fig. 9, respectively. The data were based on the fitting results from Figs. 5 and 7–8, and this comparison is to show what percentage of total swelling strain contributes to the permeability change. Although the cleat porosity term does not directly appear in the permeability model, it is included in the S_f term, $S_f = f/\phi_{f0}$, as defined in Eq. (15).
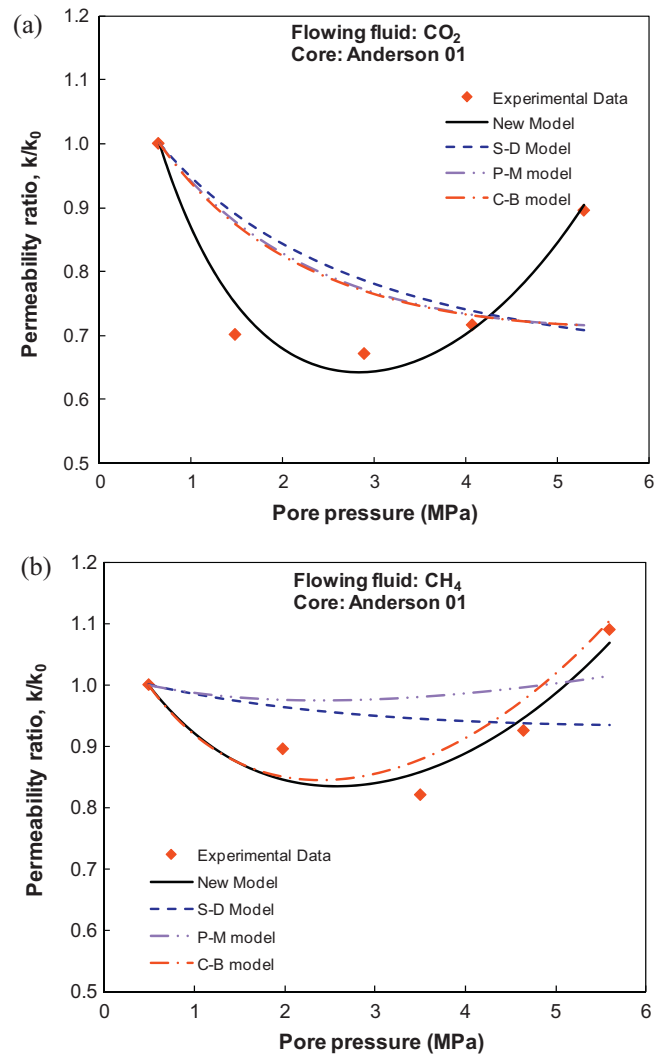

Fig. 7. Comparison of experimental permeability data (Robertson and Christiansen, 2007) with the modeled ones for core Anderson 01: (a) adsorbing gas CO_2; (b) adsorbing gas CH_4.

Table 2
Matching parameters used in the comparison of permeability models.

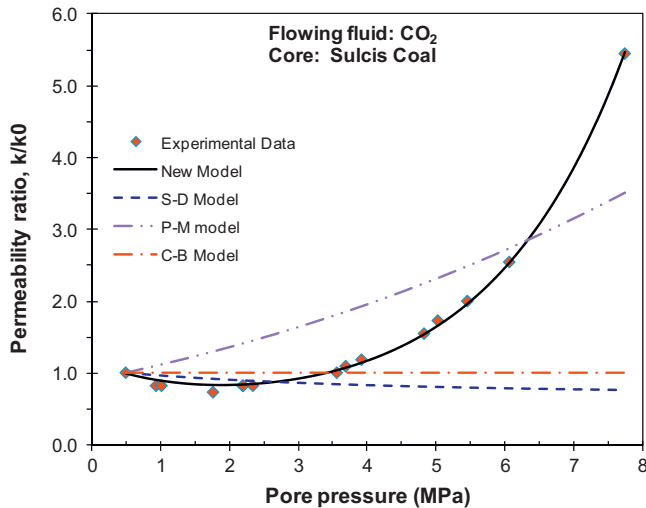| Sample	Model name				
	Physical property	S–D model	Our model	P–M model	C–B model
Anderson 01 (CO_2)	$\nu = 0.3$ $E = 1.38$ GPa	$C_f = 0.0142$ MPa^{-1}	$S_f = 35.66$ $\beta C_f = 0.0893$ MPa^{-1}	$g = 1.0$ $\Phi_{f0} = 3.18\%$	$C_f = 0.029$ MPa^{-1}
Anderson 01 (CH_4)	$\nu = 0.3$ $E = 1.38$ GPa	$C_f = 0.0101$ MPa^{-1}	$S_f = 54.78$ $\beta C_f = 0.065$ MPa^{-1}	$g = 1.0$ $\Phi_{f0} = 3.55\%$	$C_f = 0.165$ MPa^{-1}
Sulcis coal (CO_2)	$\nu = 0.26$ $E = 1.12$ GPa	$C_f = 0.01$ MPa^{-1}	$S_f = 36.78$ $\beta C_f = 7.63$ MPa^{-1}	$g = 1.0$ $\Phi_{f0} = 1.0\%$	$C_f = 0.001$ MPa^{-1}

Fig. 8. Comparison of experimental permeability data (Pini et al., 2009) with the modeled ones for core Sulcis.

Table 3
Data for porosity and partition ratio.

Porosity (%)	Partition ratio (f)		
	Core No.01 (CO_2)	Anderson 01 (CH_4)	Sulcis Coal
1.7	0.169	0.931	0.625
1.5	0.149	0.822	0.552
1.3	0.129	0.712	0.478
1.1	0.109	0.603	0.405
0.9	0.089	0.493	0.331
0.7	0.070	0.383	0.257
0.5	0.050	0.274	0.184
0.3	0.030	0.164	0.110
0.1	0.010	0.055	0.037
0.08	0.008	0.044	0.029
0.06	0.006	0.033	0.022
0.04	0.004	0.022	0.015
0.02	0.002	0.011	0.007

As demonstrated in Fig. 9, the partition ratio is linearly related to cleat porosity change. Larger cleat porosity value is accompanied by a higher partition ratio, which means more total swelling strain is absorbed by the cleat aperture system. For instance, when the cleat porosity is 1.0%, there is 54.78% of swelling strain contributing to
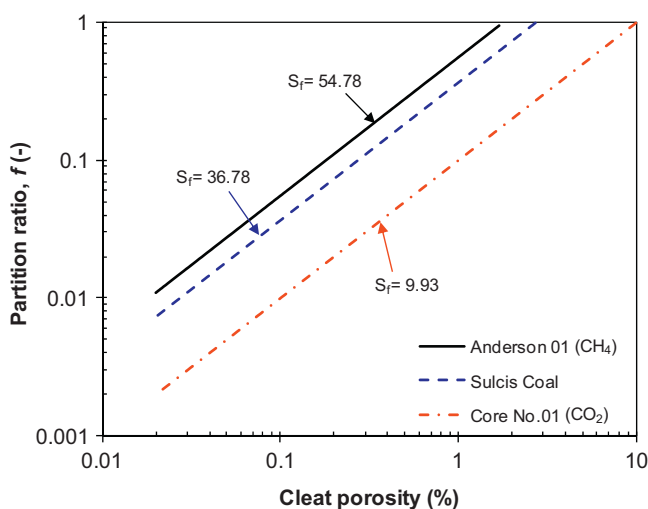

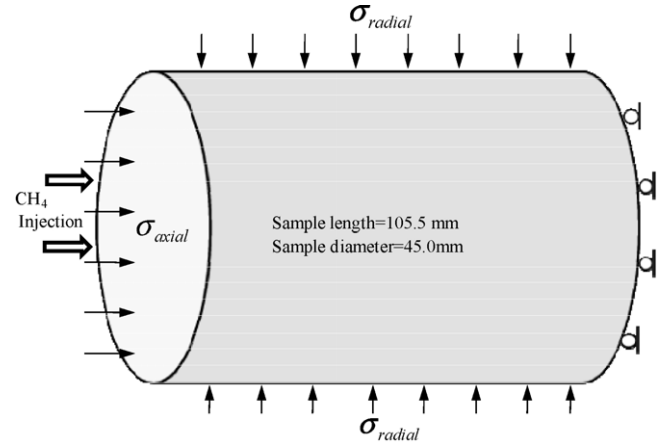Fig. 9. Partition ratio of total sorption-induced strain vs. cleat porosity.

Fig. 10. Numerical simulation model under controlled stress conditions. σ_{axial} and σ_{radial} represent the applied stress in axial and redial directions, respectively. The symbols on the right hand side represent that the deformation in the horizontal direction is constrained.

cleat aperture change, but this partition ratio decreases to 5.478% when the cleat porosity reduces to 0.1%.

All three sets of matches have illustrated that using the total swelling strain to calculate the permeability change could dramatically overestimate its contribution, which clearly demonstrates the contribution of this work.

4. Model implementation

In our previous studies (Zhang et al., 2008; Chen et al., 2009, 2010; Liu et al., 2010a, 2010b; Wu et al., 2010, 2011), a series of single poroelastic, equivalent poroelastic, and dual poroelastic models were developed to simulate the interactions of multiple processes triggered by the injection or production of both single gas and binary gas. Many studies have also been carried out by other researchers (Cui et al., 2007; Bustin et al., 2008). In order to reproduce the typical enigmatic behaviors of coal permeability evolution with gas injection, we applied the new developed permeability model to a coupled 3D finite element numerical model to simulate the performance of CH_4 injection under stress-controlled conditions.

4.1. Model descriptions

This numerical model fully couples coal geomechanical deformation, gas flow, and gas adsorption/desorption induced coal matrix swelling/shrinkage processes (see Liu et al. (2010b) for details). The core size is 45.0 mm in diameter and 105.5 mm in length with CH_4 injection at the left-hand side. Coal is initially saturated with CH_4 with pressure of 0.5 MPa. A constant injection pressure boundary condition is specified from the left side with the value of 7.0 MPa, as shown in Fig. 10. Input parameters for this simulation are listed in Table 4.

This example is to investigate the sensitivity of transient permeability with CH_4 injection to different coal physical properties as well as sorption parameters, and a series of injection conditions was simulated as listed in Table 5. Simulation results were presented in terms of (1) impacts of confining stress, (2) impacts of swelling strain, (3) impacts of fracture compressibility, (4) impacts of effective stress coefficient, and (5) impacts of sensitivity factor. A reference point with the coordinate (80 mm, 0, 0) started from the injection side was chosen to study the evolution of coal permeability and pore pressure in terms of different coal parameters. Simulation results were presented in Figs. 11–15.
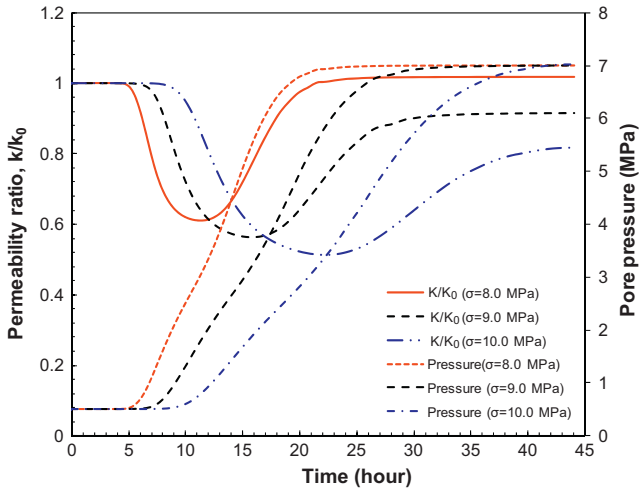
Fig. 11. Evolution of coal permeability and pore pressure under different magnitudes of confining stresses.
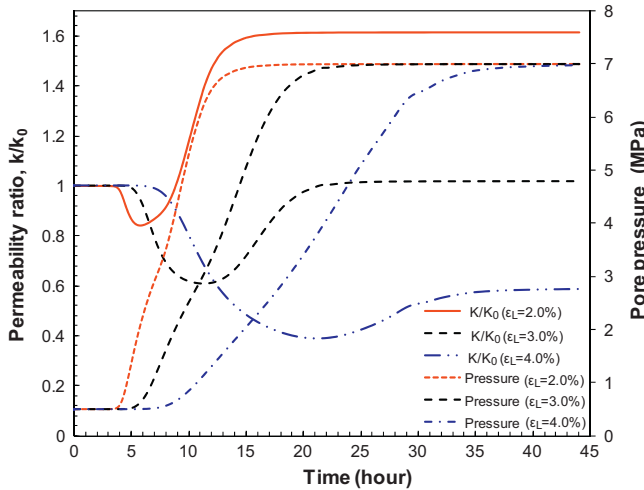

Fig. 12. Evolution of coal permeability and pore pressure under different magnitudes of the maximum volumetric swelling strain constant.

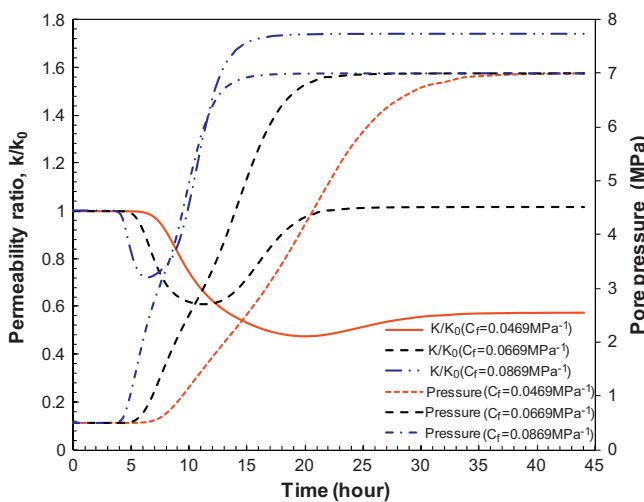**Fig. 13.** Evolution of coal permeability and pore pressure under different magnitudes of fracture compressibility.

Table 4
Input property values for the numerical model.

Parameter	Value
Coal density (kg/m^3)	1250
Coal Young's modulus (GPa)	0.791
Poisson's ratio	0.418
Effective stress coefficient	0.945
Fracture compressibility (MPa^{-1})	0.0669
Methane viscosity (μPa^{-1})	11.554
Initial gas pressure (MPa)	0.5
Maximum volumetric swelling strain	0.03
Maximum adsorption gas volume (m^3/ton)	27.0
Langmuir pressure constant (MPa)	2.96
Coal matrix porosity (%)	5.0
Coal fracture porosity (%)	0.5
Initial permeability (md)	1.0
Sensitivity factor (S_f)	30.0

4.2. Simulation results and analysis

Impact of confining stress. The impact of confining stress on the evolution of coal permeability is shown in Fig. 11. Different confining stresses represent different coal seam depth, which can be obtained by multiplying the stress gradient with the reservoir depths. Assuming the gas pressure is applied on non-adsorbing coal medium, the effective stress increases with increasing confining stress. Therefore, more reduction in coal permeability is achieved when the confining stress is higher. However, this initial effect has been eliminated when we plot the permeability ratio starting from 1.0 for all three cases. Assuming the same gas pressure condition is applied to an adsorbing coal, the sensitivities of coal permeability are regulated by the initial effective stress when coal swelling parameters are maintained unchanged. Therefore, when the confining stress is equal to 10 MPa, the reduction in coal permeability is more significant, as shown in Fig. 11.

Impact of swelling capacity. Studies from Robertson (2005) have shown that there is large difference between the strains induced by adsorption of different gases in coals, as illustrated in Fig. 3. Different maximum volumetric swelling strains used in this study represent different gas adsorbed into coal. The influence of coal maximum swelling strain on the evolution of both permeability and pore pressure were shown in Fig. 12. In all of these simulations, the initial effective stress is same for all cases. Therefore, we can assume that when gas pressure is applied in an adsorbing coal, the sensitivities of coal permeability are regulated by the maximum swelling strain only. Model results suggest that for coal seam with a

Table 5
Sensitivity investigation of permeability and pore pressure responses to CH_4 injection under different conditions.

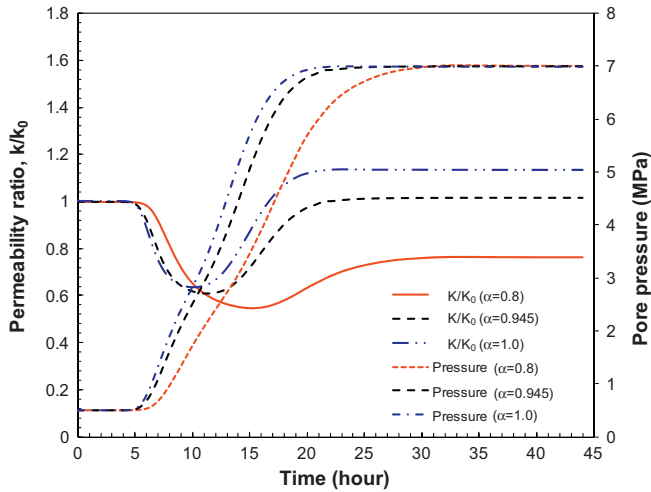|		
Case 1 Impacts of hydrostatic confining stress		$\sigma = 8.0$ MPa $\sigma = 9.0$ MPa $\sigma = 10.0$ MPa
Case 2 Impacts of swelling strain		$\varepsilon_L = 2.0\%$ $\varepsilon_L = 3.0\%$ $\varepsilon_L = 4.0\%$
Case 3 Impacts of fracture compressibility		$C_f = 0.0469$ MPa^{-1} $C_f = 0.0669$ MPa^{-1} $C_f = 0.0869$ MPa^{-1}
Case 4 Impacts of effective stress coefficient		$\alpha = 0.8$ $\alpha = 0.914$ $\alpha = 1.0$
Case 5 Impacts of sensitivity factor		$S_f = 15$ $S_f = 30$ $S_f = 45$

Fig. 14. Evolution of coal permeability and pore pressure under different magnitudes of coal effective stress coefficient.

larger swelling capacity, the reduction in coal permeability is much more significant, and this reduction in turn affects the pore pressure evolution.

Impact of fracture compressibility. The impact of compressibility is shown in Fig. 13. When the confining stress is kept as constant, both the effective stress effect and the swelling strain effect are defined as a function of gas pressure. In this set of simulations, the contribution of the effective stress to the enhancement in coal permeability is determined by coal compressibility because the swelling factor, S_f, is kept unchanged. When C_f is higher, the permeability enhancement takes over the permeability reduction. Model results are consistent with these conceptual analyses.

Impact of effective stress coefficient. Fig. 14 shows the profiles of permeability evolution with different effective stress coefficients. Based on the effective stress principle, effective stress increases as the effective stress coefficient decreases. Therefore, a smaller effective stress coefficient will result in a larger reduction in the coal permeability.

When the gas pressure is applied in an adsorbing and swelling coal, the sensitivities of coal permeability are regulated by the initial effective stress coefficient when coal swelling parameters are maintained unchanged. Therefore, when the effective stress

coefficient is equal to 0.8, more reduction in coal permeability is observed, as demonstrated in Fig. 14.

Impact of sensitivity factor. The impact of sensitivity factor is shown in Fig. 15. As stated before, S_f represents the ratio of fracture aperture strain to swelling strain incremental. When the confining stress is kept constant, both the effective stress effect and the swelling strain effect are defined as a function of gas pressure. In this example, the contribution of the swelling strain to the reduction in coal permeability is determined by the sensitivity factor, S_f. When S_f is higher, the permeability reduces more. Model results are consistent with these conceptual analyses.

5. Conclusions

Coal permeability models are required to define the transient characteristics of permeability evolution in fractured coals. A broad variety of models have evolved to represent the effects of sorption, swelling and stresses on the dynamic evolution of permeability. These models can be classified into two groups: permeability models under conditions of uniaxial strain such as Palmer–Mansoori (P–M), Shi–Durucan (S–D) and Cui–Bustin (C–B) models, and permeability models under conditions of variable stress such as the one developed in this study. Although laboratory experiments are conducted under controlled conditions of stresses, analyses of laboratory observations are normally conducted by using permeability models under conditions of uniaxial strain. The inconsistency between experimental conditions and modeling conditions is the reason why permeability models under conditions of uniaxial strain cannot match the laboratory observations well as demonstrated in this study.

Permeability models under uniaxial strain are more appropriate for the overall behavior of coal gas reservoirs under typical in situ conditions while models representing variable stress conditions are more appropriate for behavior examined under typical laboratory conditions. In this study, a phenomenological permeability model has been developed to explain why coal permeability decreases even under the unconstrained conditions of variable stress.

Unlike permeability models under the uniaxial strain condition, this model under conditions of variable stress is effective-stress based and can be used to recover the important nonlinear responses due to the effective stress effects when mechanical influences are rigorously coupled with the gas transport system. The consistency between experimental conditions and modeling conditions is the reason why this model can match the laboratory observations reasonably well.

Our modeling results illustrate that coal permeability profiles under the controlled stress conditions are regulated by the following five factors: (1) confining stress – when coal swelling parameters remain unchanged, coal permeability profiles are regulated by the initial effective stress. Coal permeability reduces initially, recovers and then reaches the final equilibrium magnitude. When the confining stress is higher, the final equilibrium coal permeability is much lower than the initial permeability; (2) swelling capacity – when confining stress conditions remain unchanged, coal permeability profiles are regulated by coal swelling capacity. Coal permeability reduces initially, recovers and then reaches the final equilibrium magnitude. When the swelling capacity is higher, the final equilibrium coal permeability is much lower than the initial permeability; (3) fracture compressibility – when the confining stress is kept as constant, both the effective stress effect and the swelling strain effect are defined as a function of gas pressure. Under these conditions, when the facture compressibility is higher, the permeability enhancement due to the decrease in effective stress may take over the permeability reduction due to swelling; (4) effective stress coefficient – the reduction in coal permeability is larger when the effective stress coefficient is
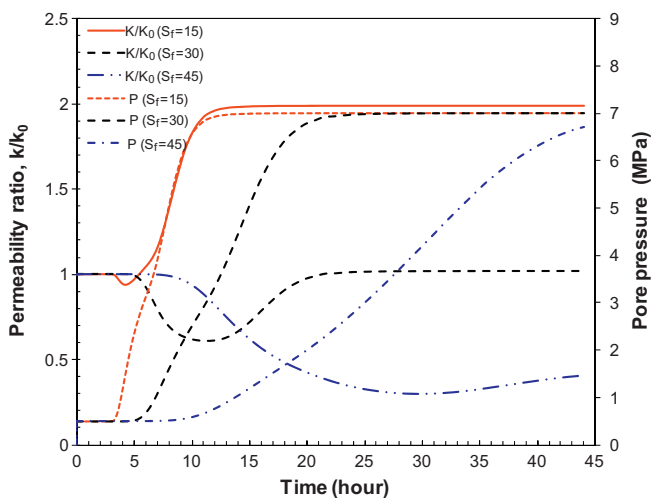

Fig. 15. Evolution of coal permeability and pore pressure under different magnitudes of sensitivity factor.

lower because the effective stress increases as the effective stress coefficient decreases; and (5) sensitivity factor – the sensitivity factor represents the ratio of fracture aperture strain to swelling strain incremental. When the sensitivity factor is higher, the reduction in coal permeability is more significant.

This study demonstrated the crucial role of the consistency between experimental conditions and modeling conditions and the rigorous coupling between coal mechanical deformation and gas transport in the evaluation of coal permeability observations.

Acknowledgments

References

Berryman, J.G., 2006. Estimates and rigorous bounds on pore-fluid enhanced shear modulus in poroelastic media with hard and soft anisotropy. International Journal of Damage Mechanics 15, 133–167.

Bustin, R.M., Cui, X., Chikatamarla, L., 2008. Impacts of volumetric strain on CO_2 sequestration in coals and enhanced CH_4 recovery. AAPG Bulletin 92, 15–29.

Chen, Z., Liu, J., Connell, L., Pan, Z., Zhou, L., 2008. Impact of effective stress and CH_4–CO_2 counter-diffusion on CO_2 enhanced coalbed methane recovery. In: SPE Asia Pacific Oil and Gas Conference and Exhibition, Perth, Australia.

Chen, Z., Liu, J., Elsworth, D., Connell, L., Pan, Z., 2009. Investigation of CO_2 injection induced coal–gas interactions. In: 43rd U.S. Rock Mechanics Symposium and 4th U.S. Canada Rock Mechanics Symposium, American Rock Mechanics Association, Asheville, NC.

Chen, Z., Liu, J., Elsworth, D., Connell, L.D., Pan, Z., 2010. Impact of CO_2 injection and differential deformation on CO_2 injectivity under in situ stress conditions. International Journal of Coal Geology 81, 97–108.

Chen, Z., Pan, Z., Liu, J., Connell, D.L., Elsworth, D., 2011. Effect of the effective stress coefficient and sorption-Induced strain on the evolution of coal permeability: experimental observations. International Journal of Greenhouse Gas Control 5, 1284–1293.

Clarkson, C.R., 2008. Case study: production data and pressure transient analysis of Horseshoe Canyon CBM Wells. In: CIPC/SPE Gas Technology Symposium 2008 Joint Conference, Society of Petroleum Engineers, Calgary, Alberta, Canada.

Connell, L.D., 2009. Coupled flow and geomechanical processes during gas production from coal seams. International Journal of Coal Geology 79, 18–28.

Connell, L.D., Lu, M., Pan, Z., 2010. An analytical coal permeability model for tri-axial strain and stress conditions. International Journal of Coal Geology 84, 103–114.

Cui, X., Bustin, R.M., Chikatamarla, L., 2007. Adsorption-induced coal swelling and stress: implications for methane production and acid gas sequestration into coal seams. Journal of Geophysics Research 112, B10202.

Cui, X., Bustin, R.M., 2005. Volumetric strain associated with methane desorption and its impact on coalbed gas production from deep coal seams. AAPG Bulletin 89, 1181–1202.

Daley, T.M., Schoenberg, M.A., Rutqvist, J., Nihei, K.T., 2006. Fractured reservoirs: an analysis of coupled elastodynamic and permeability changes from pore-pressure variation. Geophysics 71, O33–O41.

Freed, A.D., 1995. Natural strain. Journal of Engineering and Material Technology 117, 379–385.

Gilman, A., Beckie, R., 2000. Flow of coal-bed methane to a gallery. Transport in Porous Media 41, 1–16.

Gray, I., 1987. Reservoir engineering in coal seams. Part 1. The physical process of gas storage and movement in coal seams. SPE Reservoir Engineering 2, 28–34.

Harpalani, S., Chen, G., 1997. Influence of gas production induced volumetric strain on permeability of coal. Geotechnical and Geological Engineering 15, 303–325.

Harpalani, S., Schraufnagel, R.A., 1990. Shrinkage of coal matrix with release of gas and its impact on permeability of coal. Fuel 69, 551–556.

Izadi, G., Wang, S., Elsworth, D., Liu, J., Wu, Y., Pone, D., 2011. Permeability evolution of fluid-infiltrated coal containing discrete fractures. International Journal of Coal Geology 85, 202–211.

Jaeger, J.C., Cook, N.G.W., Zimmerman, R.W., 2007. Fundamentals of rock mechanics, 4th ed. Blackwell, Oxford.

Liu, H.-H., Rutqvist, J., 2010. A new coal-permeability model: internal swelling stress and fracture–matrix interaction. Transport in Porous Media 82, 157–171.

Liu, H.-H., Rutqvist, J., Berryman, J.G., 2009. On the relationship between stress and elastic strain for porous and fractured rock. International Journal of Rock Mechanics and Mining Sciences 46, 289–296.

Liu, J., Elsworth, D., Brady, B.H., 1999. Linking stress-dependent effective porosity and hydraulic conductivity fields to RMR. International Journal of Rock Mechanics and Mining Sciences 36, 581–596.

Liu, J., Chen, Z., Elsworth, D., Miao, X., Mao, X., 2010a. Evaluation of stress-controlled coal swelling processes. International Journal of Coal Geology 83, 446–455.

Liu, J., Chen, Z., Elsworth, D., Miao, X., Mao, X., 2010b. Linking gas-sorption induced changes in coal permeability to directional strains through a modulus reduction ratio. International Journal of Coal Geology 83, 21–30.

Liu, J., Chen, Z., Elsworth, D., Qu, H., Chen, D., 2011. Interactions of multiple processes during CBM extraction: a critical review. International Journal of Coal Geology 87, 175–189.

Ma, Q., Harpalani, S., Liu, S., 2011. A simplified permeability model for coalbed methane reservoirs based on matchstick strain and constant volume theory. International Journal of Coal Geology 85, 43–48.

Massarotto, P., Golding, S.D., Rudolph, V., 2009. Constant volume CBM reservoirs: an important principle. In: International Coalbed Methane Symposium, Tuscaloosa, Alabama.

Mavko, G., Jizba, D., 1991. Estimating grain-scale fluid effects on velocity dispersion in rocks. Geophysics 56, 1940–1949.

McKee, C.R., Bumb, A.C., Koenig, R.A., 1988. Stress-dependent permeability and porosity of coal and other geologic formations. SPE Formation Evaluation 3, 81–91.

Palmer, I., Mansoori, J., 1996. How permeability depends on stress and pore pressure in coalbeds: a new model. In: SPE Annual Technical Conference and Exhibition. Society of Petroleum Engineers, Inc., Denver, CO.

Palmer, I.D., Mavor, M., Gunter, B., 2007. Permeability changes in coal seams during production and injection. In: International Coalbed Methane Symposium University of Alabama, Tuscaloosa, Alabama, Paper 0713.

Pan, Z., Connell, L.D., 2007. A theoretical model for gas adsorption-induced coal swelling. International Journal of Coal Geology 69, 243–252.

Pan, Z., Connell, L.D., 2011a. Modelling of anisotropic coal swelling and its impact on permeability behaviour for primary and enhanced coalbed methane recovery. International Journal of Coal Geology 85, 257–267.

Pan, Z., Chen, Z., Connell, L.D., Lupton, N., 2011b. Laboratory characterisation of fluid flow in coal for different gases at different temperatures. In: Asia Pacific Coalbed Methane Symposium, Brisbane, Australia.

Pekot, L.J., Reeves, S.R., 2002. Modeling the Effects of Matrix Shrinkage and Differential Swelling on Coalbed Methane Recovery and Carbon Sequestration. U.S. Department of Energy, DE-FC26-00NT40924.

Pini, R., Ottiger, S., Burlini, L., Storti, G., Mazzotti, M., 2009. Role of adsorption and swelling on the dynamics of gas injection in coal. Journal of Geophysics Research 114, B04203.

Robertson, E.P., 2005. Modeling permeability in coal using sorption-induced strain data. In: SPE Annual Technical Conference and Exhibition. Society of Petroleum Engineers, Dallas, TX.

Robertson, E.P., Christiansen, R.L., 2006. A permeability model for coal and other fractured, sorptive-elastic media. In: SPE Eastern Regional Meeting. Society of Petroleum Engineers, Canton, OH, USA.

Robertson, E.P., Christiansen, R.L., 2007. Modeling laboratory permeability in coal using sorption-induced strain data. SPE Reservoir Evaluation and Engineering 10, 260–269.

Sawyer, W.K., Paul, G.W., Schraufnagel, R.A., 1990. Development and application of a 3D coalbed simulator. In: International Technical Meeting Hosted Jointly by the Petroleum Society of CIM and the Society of Petroleum Engineers, Calgary, Alberta, Canada, CIM/SPE 90-1119.

Seidle, J.R., Huitt, L.G., 1995. Experimental measurement of coal matrix shrinkage due to gas desorption and implications for cleat permeability increases. In: International Meeting on Petroleum Engineering. Society of Petroleum Engineers, Inc., Beijing, China.

Shi, J.Q., Durucan, S., 2004. Drawdown induced changes in permeability of coalbeds: a new interpretation of the reservoir response to primary recovery. Transport in Porous Media 56, 1–16.

Shi, J.-Q., Durucan, S., 2010. Exponential growth in San Juan Basin Fruitland coalbed permeability with reservoir drawdown: model match and new insights. SPE Reservoir Evaluation and Engineering 13, 914–925.

Somerton, W.H., Söylemezoglu, I.M., Dudley, R.C., 1975. Effect of stress on permeability of coal. International Journal of Rock Mechanics and Mining Sciences and Geomechanics 12, 129–145 (Abstracts).

Tonnsen, R.R., Miskimins, J.L., 2010. Simulation of deep coalbed methane permeability and production assuming variable pore volume compressibility. In: Canadian Unconventional Resources and International Petroleum Conference, Calgary, Alberta, Canada.

White, C.M., Smith, D.H., Jones, K.L., Goodman, A.L., Jikich, S.A., LaCount, R.B., DuBose, S.B., Ozdemir, E., Morsi, B.I., Schroeder, K.T., 2005. Sequestration of carbon dioxide in coal with enhanced coalbed methane recoverys-a review. Energy and Fuels 19, 6–7.

Wu, Y., Liu, J., Chen, Z., Elsworth, D., Pone, D., 2011. A dual poroelastic model for CO_2-enhanced coalbed methane recovery. International Journal of Coal Geology 86, 177–189.

Wu, Y., Liu, J., Elsworth, D., Chen, Z., Connell, L., Pan, Z., 2010. Dual poroelastic response of a coal seam to CO_2 injection. International Journal of Greenhouse Gas Control 4, 668–678.

Zhang, H., Liu, J., Elsworth, D., 2008. How sorption-induced matrix deformation affects gas flow in coal seams: a new FE model. International Journal of Rock Mechanics and Mining Sciences 45, 1226–1236.